Journal of Biological Dynamics
iFirst, 2011, 1–17

A mathematical model for cell cycle-specific cancer virotherapy

Joseph J. Crivelli[a]*, Juraj Földes[a], Peter S. Kim[b] and Joanna R. Wares[c]

[a]*Department of Mathematics, Vanderbilt University, Nashville, TN 37240, USA;* [b]*School of Mathematics and Statistics, University of Sydney, NSW 2006, Australia;* [c]*Department of Math and Computer Science, University of Richmond, Richmond, VA 23173, USA*

(*Received 6 October 2010; final version received 5 August 2011*)

Oncolytic viruses preferentially infect and replicate in cancerous cells, leading to elimination of tumour populations, while sparing most healthy cells. Here, we study the cell cycle-specific activity of viruses such as vesicular stomatitis virus (VSV). In spite of its capacity as a robust cytolytic agent, VSV cannot effectively attack certain tumour cell types during the quiescent, or resting, phase of the cell cycle. In an effort to understand the interplay between the time course of the cell cycle and the specificity of VSV, we develop a mathematical model for cycle-specific virus therapeutics. We incorporate the minimum biologically required time spent in the non-quiescent cell cycle phases using systems of differential equations with incorporated time delays. Through analysis and simulation of the model, we describe how varying the minimum cycling time and the parameters that govern viral dynamics affect the stability of the cancer-free equilibrium, which represents therapeutic success.

Keywords: oncolytic virus; VSV; cell cycle; time delay; age structure; ratio dependence

1. Introduction

The efficacy of cancer treatment has improved dramatically in the last decade. However, patients with certain forms of cancer are still left with limited options for therapy. Many tumours also remain completely incurable, creating a need for a broader spectrum of therapeutic strategies. One promising form of treatment is oncolytic virotherapy. This technique employs replication-competent viral vectors as agents that preferentially attack and proliferate in cancerous cells, leaving most healthy cells uninjured. The result is the destruction of tumour populations without appreciable damage to normal tissue. There are many oncolytic viruses which have demonstrated anti-tumour efficacy, including adenoviruses [14], Coxsackieviruses [1], herpes simplex viruses [26], measles viruses [11], Newcastle disease virus [22], reoviruses [10], Seneca Valley virus [24], vaccinia viruses [21], and vesicular stomatitis virus (VSV) [6].

*Corresponding author. Email: joseph.j.crivelli@vanderbilt.edu
Author Emails: juraj.foldes@vanderbilt.edu; kim@math.utah.edu; jwares@richmond.edu

ISSN 1751-3758 print/ISSN 1751-3766 online

http://dx.doi.org/10.1080/17513758.2011.613486
http://www.tandfonline.com

Mathematical modelling of cancer treatment can illuminate the underlying dynamics of therapy systems and can lead to more optimal treatment strategies. A wide variety of virotherapy models have been proposed which consider spatial representation of tumours [13,29,31], multi-scale effects [20] and stochastic processes [25]. A number of models have been developed and analysed based on population dynamics of tumour cells subjected to virotherapy treatment [3,15,18,30]. A defining feature of these ordinary differential equation (ODE) models is the compartmentalization of uninfected tumour, infected tumour, and free virus populations. The lytic activity of viral particles is also a fundamental component. Several models have been custom tailored to certain viruses for the purpose of developing optimal therapy schedules [2,8]. Findings of these studies have recapitulated that each candidate virus has unique oncolytic dynamics, leading to a unique treatment plan. Therefore, it remains essential to develop models in order to understand the therapeutic impact of such dynamics for individual viral vectors.

In this paper, we develop a mathematical model for the cell cycle-specific activity of the oncolytic VSV therapeutic. VSV is an RNA virus which has demonstrated anti-tumour efficacy in a large panel of human tumour cell lines, including prostate, breast, cervical, and haematologic cancers [4]. Importantly, it has oncolytic activity in several tumour cell types that are resistant to chemotherapy [4]. The efficacy of VSV has been attributed to a defective antiviral interferon response in tumours, leading to preferential attack and replication in cancerous cells [5].

A distinguishing characteristic of VSV is its inability to replicate in leukemic T-lymphocytes in the quiescent (resting) phase of the cell cycle known as G_0 [19]. This renders quiescent cells resistant to VSV treatment, while cycling cells remain susceptible. We know of no model of virotherapy that accounts for cycle specificity of the viral agent; however, models have been developed for cancer treatment with cycle specific chemotherapy agents [16,28]. These models compartmentalize the phases of the cell cycle for the study of the therapeutic agent's action on cancerous cells throughout the different phases. Delay differential equations (DDE) are then utilized to account for the minimum biological time course of certain phases.

In a similar fashion to two of the chemotherapy models, Villasana and Radunskaya [28] and Liu *et al.* [16], we separate cycling and quiescent cell populations into compartments and account for the minimum time course of the active phases of the cell cycle. To incorporate virotherapy, we also separate cycling cells into infected and uninfected compartments and model the viral lytic cycle, which includes virus-uninfected cell contact and the release of viral particles upon death of infected cells. Without taking into account the time delay, virotherapy is modelled as in Bajzer *et al.* [2]. However, once the minimum time course of the active phases of the cell cycle are incorporated, the complexities of these virus-cell interactions require a system that includes an age-structured partial differential equation (PDE). Previous authors have developed models for chronic myelogenous leukaemia in which age structure accounts for time spent in the cell cycle [9,23]. Likewise, we utilize age structure to account for the temporal dynamics of the cell cycle. Figure 1 provides a schematic of our full model.

Close inspection of the models created by Villasana and Radunskaya [28] and Liu *et al.* [16] reveals that there is a more correct way to properly account for decay of tumour cells. We modify the Liu *et al.* [16] model of tumour growth to properly account for cell death and viral attack during the delay period. Proper accounting of cell death is achieved through the inclusion of an additional compartment for cells which have exited G_0 and must remain in the non-resting phases for a minimum time determined by the delay value. However, during this time, cells can still die and exit the compartment. This important feature of our basic tumour growth model extends to our full virotherapy model.

In an attempt to uncover the determinants of effective virotherapy treatment with VSV, we investigate which parameters most significantly impact the stability of equilibria. We also examine how the length of the time delay and parameter values governing viral dynamics affect the stability of these steady states. Such analysis elucidates the factors that promote complete remission,

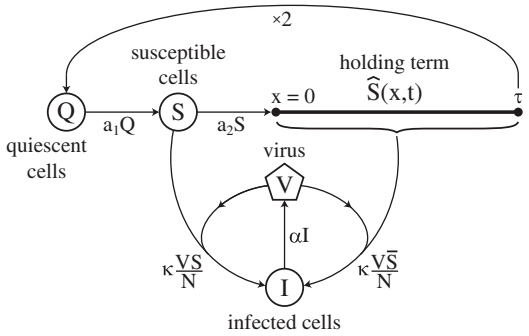

Figure 1. Compartmental diagram for the full model of virotherapy. Transfer occurs from the quiescent to the non-quiescent, or susceptible, cell population at rate a_1, and susceptible cells begin mitosis at rate a_2. Susceptitle cells remain in a holding state for at least τ units of time. After completing mitosis, two daughter cells enter the quiescent population. Susceptible cells are infected through contact with the free virus population at rate $\kappa V/N$ and enter the infected state. Viral reproduction in infected cells, combined with lysis, leads to production of free virions at a rate α. Although not shown in the diagram, all cell and virus populations, Q, S, $\hat{S}$, I, and V die or decay at rates d_1, d_2, d_3, δ, and ω, respectively.

limitation of tumour growth, or uncontrolled tumour growth. Additionally, we perform numerical simulations of the full virotherapy model for additional analysis of fixed points and parameter interaction.

2. Mathematical model and stability results

We incrementally develop our mathematical model. The first step is the analysis of a simple two-dimensional ODE model for tumour growth. We then consider a three-dimensional DDE model for tumour growth and analyse delay effects in the absence of therapy. Following this, we again exclude the time delay and extend the two-dimensional ODE model to include virotherapy, resulting in a four-dimensional system of ODEs. Finally, the inclusion of a time delay yields our complete model: a five-dimensional cycle-specific age-structured model for virotherapy treatment with VSV.

2.1. *The virus-free system*

Our model for tumour growth in the absence of therapy contains parameters determining the rates of cell division, death, and transfer between resting and active states of the cell cycle, and later, the added delay parameter. The analysis aims to predict how these parameters impact achievement of a tumour-free state without therapy. These findings will be important for comparative purposes when analysing our model with therapy.

2.1.1. *Non-delay case*

We are interested in studying the case where VSV cannot attack tumour cells in the resting phase known as G_0, but can infect cells in all other phases. Therefore, we partition tumour cells into two populations: Q (quiescent) – volume of cells in the quiescent or resting stage of the cell cycle, and S (susceptible) – volume of cells in all other phases of the cell cycle, including stages of growth, DNA synthesis, and mitosis. In the absence of virotherapy treatment and a time delay, we are left with a simple two-dimensional linear system of ODEs. The asymptotic behaviour of

any trajectory is either exponential growth or decay to the origin. The conditions for stability and instability of the cancer-free equilibrium (CFE), $(Q, S) = (0, 0)$, are determined using linear systems theory. The governing equations are as follows:

$$Q'(t) = 2a_2S - a_1Q - d_1Q, \tag{1}$$

$$S'(t) = a_1Q - a_2S - d_2S. \tag{2}$$

Cells leave Q and enter S at a rate of a_1. Natural cell death occurs in Q at a rate of d_1 and in S at a rate of d_2. After mitosis, two daughter cells emerge from S and enter the the quiescent state, Q; hence the term $2a_2S$. Note that it is possible for cells to immediately exit back into S.

The eigenvalues of the corresponding Jacobian matrix about $(Q, S) = (0, 0)$ are

$$\lambda_{1,2} = \frac{-(a_1 + a_2 + d_1 + d_2) \pm \sqrt{(a_1 + a_2 + d_1 + d_2)^2 - 4(a_1(d_2 - a_2) + d_1(a_2 + d_2))}}{2}.$$

Here we know both eigenvalues are always real when all parameters are non-negative, since,

$$\begin{aligned}&(a_1 + a_2 + d_1 + d_2)^2 - 4(a_1(d_2 - a_2) + d_1(a_2 + d_2))\\ &\quad = d_1^2 + (a_1 + a_2 + d_2)^2 - 2d_1(a_1 + a_2 + d_2) + 4a_1a_2,\end{aligned}$$

and it follows from the Cauchy–Schwarz inequality that

$$d_1^2 + (a_1 + a_2 + d_2)^2 \geq 2d_1(a_1 + a_2 + d_2).$$

Therefore, if $a_1(d_2 - a_2) + d_1(a_2 + d_2) > 0$, both eigenvalues are negative and the CFE is stable, implying that the tumour would naturally be eradicated. Contrarily, if $a_1(d_2 - a_2) + d_1(a_2 + d_2) < 0$, then one eigenvalue is positive, the CFE is unstable, and the tumour grows exponentially. Notice that if either $d_1 > a_1$ or $d_2 > a_2$ (either compartment has a death rate which dominates the corresponding rate of transfer within the system), then the CFE is stable. We note that these results are analogous to those of Villasana and Radunskaya [28].

2.1.2. *Delay case*

The previous model of exponential tumour growth and death did not fully account for several time-consuming processes of the cell cycle. In this section, we add a delay which reflects the minimum time required to complete DNA replication, mitosis, and their requisite metabolic processes. The duration of these processes varies, but there is a minimum, biologically required amount of time, τ, to complete them. Studies of a broad array of human solid tumour types revealed that cell cycle progression lasts 2 days, on average [27]. The model in the previous section did not account for a minimum time for cycle completion, allowing cells that entered S to immediately exit. In the following model, we force cells that enter the susceptible state to remain there for at least τ days. The model equations are

$$Q'(t) = 2a_2\,\mathrm{e}^{-d_3\tau}S(t - \tau) - a_1Q - d_1Q, \tag{3}$$

$$S'(t) = a_1Q - a_2S - d_2S, \tag{4}$$

$$\bar{S}'(t) = a_2S - d_3\bar{S} - a_2\,\mathrm{e}^{-d_3\tau}S(t - \tau), \tag{5}$$

with history functions given by $Q(t) = \phi_q(t)$, $S(t) = \phi_s(t)$ and $\bar{S}(t) = \phi_{\bar{s}}(t)$, for $-\tau \leq t \leq 0$.

The state $\bar{S}$ represents the volume of susceptible cells which are committed to completing the necessary biological processes of the active phases of the cell cycle. Notice that Equations (3) and

(4) do not contain the variable $\bar{S}$. Here, the compartment $\bar{S}$ is used only for book-keeping purposes; that is, to determine the total volume of cells that are susceptible ($S + \bar{S}$). Our model improves upon previous models of tumour growth by properly factoring in cell death during the delay period. As indicated in Liu *et al.* [16], the model developed by Villasana and Radunskaya [28] removes cells from interphase at time t based on how many cells there were τ days ago, without accounting for the amount of these cells that have naturally died since then. This can lead to solutions that become negative. Additionally, all cells that leave the interphase immediately enter mitosis, and because natural death is not accounted for, too many cells enter mitosis. The latter issue remained in the model proposed by Liu *et al.* [16], where the proper amount of cells is removed from interphase and positivity of solutions is guaranteed. But, as in the case of Villasana and Radunskaya [28], death is not accounted for during the delay period, resulting in the passage of too many cells into mitosis; therefore, tumour populations are, in general, overstated.

To properly account for cell death during the minimum time period in the non-resting phases, τ, the rate that cells enter Q should be proportional to the amount of cells that were in the S state τ days ago, multiplied by a factor which represents natural death (exponential decay) at a rate of d_3 per day. Thus, the term $2a_2S$ from Equation (1) is replaced by $2a_2\,\mathrm{e}^{-d_3\tau}S(t-\tau)$. Cells in S leave at a rate a_2 after being in $\bar{S}$ for the minimum amount of time, τ days, necessary to complete the non-quiescent phases. Note that we allow cells in $\bar{S}$ to die at a different rate, d_3, than those in S. It is, however, likely that $d_2 = d_3$.

The compartment $\bar{S}$ does not affect the rate of change of the Q or S populations, but to find the amount of cells in the susceptible state at any time, we add the amount of cells in S to the amount of cells in $\bar{S}$, which is determined by calculating an explicit solution for Equation (5):

$$\bar{S}(t) = \bar{S}(0)\,\mathrm{e}^{-d_3t} + a_2\,\mathrm{e}^{-d_3t}\int_{t-\tau}^{t}\mathrm{e}^{d_3u}S(u)\,\mathrm{d}u - a_2\,\mathrm{e}^{-d_3t}\int_{-\tau}^{0}\mathrm{e}^{d_3u}\phi_s(u)\,\mathrm{d}u.$$

We also assume that cells that are in the holding state before $t = -\tau$, leave before $t = 0$. Mathematically, we can do this by setting $\bar{S}(0) = a_2\int_{-\tau}^{0}\mathrm{e}^{d_3u}\phi_s(u)\,\mathrm{d}u$. In this case

$$\bar{S}(t) = a_2\,\mathrm{e}^{-d_3t}\int_{t-\tau}^{t}\mathrm{e}^{d_3u}S(u)\,\mathrm{d}u. \tag{6}$$

Furthermore, because we can explicitly solve for $\bar{S}$ in terms of S, when studying dynamics or looking for solutions, we can exclude it from the system and only consider Equations (3) and (4).

THEOREM 2.1 *Assume that $\phi_q(t)$, $\phi_s(t)$ and $\phi_{\bar{s}}(t)$ are non-negative. Then, solutions of Equations (3)–(5) are non-negative for $t > 0$.*

Proof We study the time-varying vector field in the $Q - S$ plane. Solutions starting in the first quadrant become negative by crossing either the Q-axis or the S-axis. Along the positive part of the Q-axis, $S = 0$ and $S'(t) > 0$. Therefore, the vector field points upward. As such, solutions cannot cross the positive part of the Q-axis from the first quadrant.

Assume towards a contradiction that a solution crosses the S-axis above the origin into the second quadrant for some $t \in [0, \tau)$. So for some $t_1 \in [0, \tau]$, the solution is moving to the left, $Q'(t_1) < 0$, into the second quadrant where $S > 0$ and $Q \leq 0$. But if we assume $\phi_s(t) \geq 0$, then because $S(t_1 - \tau) \geq 0$ and $Q(t_1) < 0$, $Q'(t_1)$ must be positive – a contradiction.

At the origin, solutions either remain or become positive, since S has a non-negative history function. The same is then true for $t \in [\tau, 2\tau]$. This process can be carried out *ad infinitum*, and $Q'(t)$ will never be negative. Therefore, solutions cannot cross the S-axis and will remain non-negative for all time. Note that non-negativity of $\bar{S}(t)$ is guaranteed since $S(t)$ remains non-negative. ■

The system consisting of Equations (3) and (4) is linear, so the only fixed point is (0, 0), barring linear dependence of coefficients, which does not occur in the general case. The Jacobian is

$$J = \begin{bmatrix} -(a_1 + d_1) & 2a_2\, e^{-d_3\tau}\, e^{-\lambda\tau} \\ a_1 & -(a_2 + d_2) \end{bmatrix},$$

from which we derive the characteristic equation:

$$P(\lambda) = 2a_1a_2\, e^{-d_3\tau}\, e^{-\lambda\tau} - (a_1 + d_1 + \lambda)(a_2 + d_2 + \lambda) = 0. \tag{7}$$

We now investigate the stability of the CFE (0, 0), for the system of Equations (3)–(4). Our main result, given below, describes a condition on τ, which, if achieved, results in a stable CFE.

THEOREM 2.2 *For any* $a_1, a_2, d_1, d_2, d_3 > 0$, $(Q, S) = (0, 0)$ *is stable when*

$$\tau > \frac{1}{d_3} \log\left(\frac{2a_1a_2}{(a_1 + d_1)(a_2 + d_2)}\right) > 0$$

and unstable when

$$0 < \tau < \frac{1}{d_3} \log\left(\frac{2a_1a_2}{(a_1 + d_1)(a_2 + d_2)}\right).$$

Theorem 2.2 shows that for any growth and death rates, there is a τ, given by the condition in the theorem, for which the tumour would be naturally eliminated. To prove this theorem, we must first prove the following lemma.

LEMMA 2.3 *For any* $a_1, a_2, d_1, d_2, d_3 > 0$, *the rightmost eigenvalue derived from the characteristic equation* (7) *is real.*

Proof The function $P(\lambda)$ is strictly decreasing for $\lambda > -\min(a_1 + d_1, a_2 + d_2)$. Furthermore, $P(-\min(a_1 + d_1, a_2 + d_2)) > 0$ and $P(\lambda) \to -\infty$ as $\lambda \to \infty$. Hence, $P(\lambda_0) = 0$ for exactly one value of $\lambda_0 > -\min(a_1 + d_1, a_2 + d_2)$.

Suppose $\lambda_* = \lambda_r + i\lambda_i$ is any eigenvalue of Equation (7), where $\lambda_r, \lambda_i \in \mathbb{R}$. Then,

$$P(\lambda_*) = 0 \Rightarrow (a_1 + d_1 + \lambda_r + i\lambda_i)(a_2 + d_2 + \lambda_r + i\lambda_i) = 2a_1a_2\, e^{-d_3\tau}\, e^{-(\lambda_r + i\lambda_i)\tau}.$$

Taking the magnitudes of both sides of the equation, we obtain

$$\sqrt{((a_1 + d_1 + \lambda_r)^2 + \lambda_i^2)((a_2 + d_2 + \lambda_r)^2 + \lambda_i^2)} = 2a_1a_2\, e^{-d_3\tau}\, e^{-\lambda_r\tau}.$$

Since

$$(a_1 + d_1 + \lambda_r)(a_2 + d_2 + \lambda_r) \le \sqrt{((a_1 + d_1 + \lambda_r)^2 + \lambda_i^2)((a_2 + d_2 + \lambda_r)^2 + \lambda_i^2)},$$

it follows that

$$0 \le 2a_1a_2\, e^{-d_3\tau}\, e^{-\lambda_r\tau} - (a_1 + d_1 + \lambda_r)(a_2 + d_2 + \lambda_r),$$

which indicates that $P(\lambda_0) = 0 \le P(\lambda_r)$. Since $P(\lambda)$ is decreasing with respect to λ for $\lambda \ge \lambda_0$, it follows that $\mathrm{Re}(\lambda_*) = \lambda_r < \lambda_0$. Therefore, the real eigenvalue λ_0 is, indeed, the rightmost eigenvalue. ■

Having proved the previous lemma, we prove the following proposition. The theorem directly follows.

PROPOSITION 2.4 *For any parameters* a_1, a_2, d_1, d_2, $d_3 > 0$, *the CFE* $(Q, S) = (0, 0)$ *of the system of Equations* (*3*) *and* (*4*) *is globally asymptotically stable if*

$$2a_1a_2\,\mathrm{e}^{-d_3\tau} - (a_1 + d_1)(a_2 + d_2) < 0,$$

and unstable if

$$2a_1a_2\,\mathrm{e}^{-d_3\tau} - (a_1 + d_1)(a_2 + d_2) > 0.$$

Proof Recall from the first line of the proof of Lemma 2.3, that $P(\lambda)$ is strictly decreasing for $\lambda > -\min(a_1 + d_1, a_2 + d_2)$. Therefore, if

$$P(0) = 2a_1a_2\,\mathrm{e}^{-d_3\tau} - (a_1 + d_1)(a_2 + d_2) < 0,$$

then there are no non-negative real eigenvalues. By Lemma 2.3, the rightmost eigenvalue of Equation (7) is real, so all eigenvalues must have negative real parts. Hence, the CFE of system (3) and (4) is asymptotically stable. Global stability follows, since Equations (3) and (4) is linear.

On the contrary, if

$$P(0) = 2a_1a_2\,\mathrm{e}^{-d_3\tau} - (a_1 + d_1)(a_2 + d_2) > 0,$$

then there exists a positive real eigenvalue. Therefore, the CFE is unstable. ■

We note that, based on the above proposition, in the $\tau = 0$ case, the conditions for stability or instability of the origin are identical to those for the system of Equations (1) and (2). Given a_1, a_2, d_1, d_2 and d_3, it is also possible to determine a threshold delay value, about which stability switches occur. Our model for tumour growth indicates that lengthening the time spent in the active phases of the cell cycle can eradicate the tumour. In essence, the delay is reducing the growth rate by lengthening the doubling time of the tumour population. Many cancer chemotherapy agents function via similar cell cycle inhibiting effects. By arresting rapidly proliferating cells, such drugs can both reduce tumour growth rates and stimulate apoptosis due to insufficient metabolic activity.

2.2. *The virotherapy system*

In this section, we add cell cycle-specific oncolytic virotherapy to the model for tumour growth. The model will now contain an additional layer of dynamic complexity, resulting from the inclusion of free virus (V) and infected cell (I) populations, as well as the presence of a nonlinear, ratio-dependent contact term. We first consider the system without taking into account the minimum time needed to travel through the cell cycle. We then consider this effect by adding the time delay through age structure.

2.2.1. *Non-delay case*

VSV infects susceptible cells and replicates repeatedly, leading to lysis. When lysis occurs, the viral particles are free to infect other susceptible cells. Previous authors have modelled oncolytic virus infection with a mass action term, similar to many epidemic models, where the infection rate is dependent on the amount of susceptible tumour cells and the amount of virions, described mathematically by $\bar{\kappa}S(t)V(t)$, where $\bar{\kappa}$ is the rate of infection with units day^{-1} $\times$ (cells and virions)$^{-1}$ [3,30]. Mass action is an appropriate approximation when the total population of cells and virions is fairly constant, but it generally assumes that the contact rate grows as the population of virions and cells grows; that is, the density of the population is proportional to the total amount

of cells and virions [18]. When density does not change with the amount of cells or virions, it is more appropriate to use a ratio-dependent transmission term $\kappa S(t)V(t)/N(t)$, where $N(t)$ is the total amount of cells and virions. κ is equal to the probability of infection per virion contact with a susceptible cell, times the average number of contacts virions make per day with cells and virions, and has standard rate units day^{-1}. $S(t)/N(t)$ is the proportion of contacts made with susceptible cells. The ratio-dependent term is necessary to account for the likelihood that a virion will come in contact with a susceptible cell, assuming that each virion is equally likely to contact any type of cell or other virions. Of course, cells are larger than virions, but more individual virions will be nearby. In addition, even if one or several populations become arbitrarily large, the proportional infection rate will saturate to κ.

A mathematical advantage of modelling infection with ratio-dependent transmission is that the virus can affect the stability of the CFE, thereby suggesting that the virus can eliminate the tumour [18]. Contrarily, mass action dynamics cannot impact the stability of the origin. This becomes clear by inspecting the linearization of the system about the origin. The mass action term $\bar{\kappa}S(t)V(t)$ is represented in the Jacobian by either $\bar{\kappa}S(t)$ or $\bar{\kappa}V(t)$. At the origin, both of these terms are zero.

Using the ratio-dependent contact to describe viral infection, our model becomes

$$Q'(t) = 2a_2S - a_1Q - d_1Q, \tag{8}$$

$$S'(t) = a_1Q - a_2S - d_2S - \kappa\frac{VS}{N}, \tag{9}$$

$$I'(t) = \kappa\frac{VS}{N} - \delta I, \tag{10}$$

$$V'(t) = \alpha I - \kappa\frac{VS}{N} - \omega V, \tag{11}$$

where the total of amount of cells and virions, here measured by volume (mm^3), changes with time and is given by $N(t) = Q(t) + S(t) + I(t) + V(t)$.

The Q compartment is unchanged by the virus because the virus cannot infect quiescent cells. Susceptible cells become infected at a rate of κ per day, exiting S and entering I at a rate of $\kappa VS/N$ [18]. Infected cells are eliminated at a rate of δ per day by lysis due to viral replication or by the cytotoxic immune response. Lysis of infected cells releases free viral particles at a rate of α. When virions infect susceptible cells, they are removed from the free particle population, also at a rate of $\kappa VS/N$. Finally, molecular decay and immunologically mediated death of virions occurs at the rate ω.

The system above is mathematically difficult, not only due to its nonlinearities, but more importantly, because it is not C^1 at the origin. This can cause interesting dynamical behaviour [7,18,32]. It is natural to extend the system by letting the right-hand sides of Equations (8)–(11) equal zero when $(Q, S, I, V) = (0, 0, 0, 0)$. In the extended system, the origin is the only equilibrium point, but since the system is not C^1 at the origin, the system cannot be linearized there and local stability cannot be determined. For this reason, we employ numerical simulations to determine when virotherapy can act as a successful treatment, which is represented by a switch from the exponential tumour growth to a stable cancer-free state (Figure 2).

2.2.2. *Delay case*

Finally, as in Section 2.1.2, we extend our model to include the minimum time that a cell spends in the active phases of the cell cycle. In a similar fashion to our DDE model for tumour growth, we include a holding compartment in which cells committed to the active phases of the cell cycle

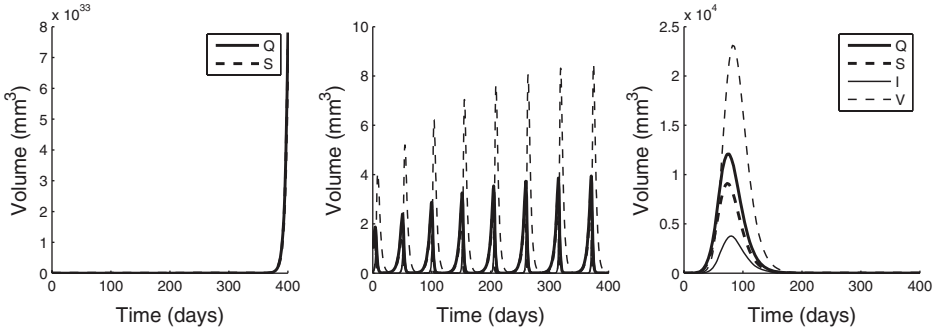

Figure 2. Tumour growth in time. Left: uncontrolled tumour growth in the absence of therapy. Middle: growing oscillatory behaviour of solutions when virus-cell contact is modelled through mass action. Right: complete tumour elimination; virus-cell contact is modelled through ratio dependence. Parameter values: $a_1 = 0.9$, $a_2 = 0.6$, $d_1 = 0.00001$, $\bar{\kappa} = 0.001$, $\kappa = 1$, $\delta = 1.119$, $\omega = 0.3$, and $\alpha = 3$.

must reside for a minimum time τ. Owing to the more complex structure of these interactions, we write the full model as a system of four ODEs and one age-structured PDE as follows:

$$\frac{\mathrm{d}Q}{\mathrm{d}t} = 2\hat{S}(\tau, t) - a_1 Q - d_1 Q, \tag{12}$$

$$\frac{\mathrm{d}S}{\mathrm{d}t} = a_1 Q - a_2 S - d_2 S - \kappa \frac{VS}{N}, \tag{13}$$

$$\frac{\partial \hat{S}}{\partial t} + \frac{\partial \hat{S}}{\partial x} = -d_3 \hat{S} - \kappa \frac{V\hat{S}}{N}, \tag{14}$$

$$\frac{\mathrm{d}I}{\mathrm{d}t} = -\delta I + \kappa \frac{VS + V\bar{S}}{N}, \tag{15}$$

$$\frac{\mathrm{d}V}{\mathrm{d}t} = \alpha I - \omega V - \kappa \frac{VS + V\bar{S}}{N}, \tag{16}$$

where $\bar{S}(t) = \int_0^\tau \hat{S}(x, t)\,\mathrm{d}x$, $N(t) = Q(t) + S(t) + \bar{S}(t) + I(t) + V(t)$, and the boundary condition is given by

$$\hat{S}(0, t) = a_2 S(t).$$

$\hat{S}$ is a function of two variables: t–time, and x–the length of time already spent in the cell cycle. Note that the PDE now accounts for the loss of susceptible cells in the delay period. For biological relevance, the initial conditions, $Q(0)$, $S(0)$, $\hat{S}(x, 0)$, $I(0)$ and $V(0)$, are all assumed to be non-negative. To extend the model to the origin, when $N = 0$, we let the right-hand sides of Equations (12)–(16) equal zero. Note that the system (12)–(16) reduces to (8)–(11) when $\tau = 0$.

If we remove virotherapy, and assume that, for $0 \le x \le \tau$, $\hat{S}(x, 0) = a_2 \phi_s(-x)\,\mathrm{e}^{-d_3 x}$ then this system acts like Equations (3)–(5). With I and V removed, $\hat{S}$ can be found using the method of characteristics,

$$\hat{S}(x, t) = \hat{S}(0, t - x)\,\mathrm{e}^{-d_3 x}.$$

We can then find $\bar{S}(t)$ noting that $\hat{S}(0, t - x) = a_2 S(t - x)$,

$$\begin{aligned}\bar{S}(t) &= \int_0^\tau \hat{S}(x, t)\,\mathrm{d}x = \int_0^\tau \hat{S}(0, t - x)\,\mathrm{e}^{-d_3 x}\,\mathrm{d}x \\ &= \int_0^\tau a_2 S(t - x)\,\mathrm{e}^{-d_3 x}\,\mathrm{d}x\end{aligned}$$

$$= \int_{t-\tau}^{t} a_2 S(u)\, \mathrm{e}^{-d_3(t-u)}\, \mathrm{d}u$$

$$= a_2\, \mathrm{e}^{-d_3 t} \int_{t-\tau}^{t} \mathrm{e}^{d_3(u)} S(u)\, \mathrm{d}u.$$

This is the same as the solution for the virus-free system, Equation (6).

Next we show that solutions remain non-negative.

THEOREM 2.5 *Assume that $Q(0)$, $S(0)$, $\hat{S}(x,0)$, $I(0)$ and $V(0)$ are non-negative. Then, solutions of the system (12)–(16) are non-negative for $t \geq 0$.*

Proof If $Q(0) = S(0) = \hat{S}(x,0) = \hat{S}(0,t) = I(0) = V(0) = 0$, then by definition $Q(t) = S(t) = \hat{S}(x,t) = I(t) = V(t) = 0$ and we are at equilibrium.

Otherwise by assumption, at $t = 0$, all compartments are greater than or equal to zero and $N(0) > 0$. In this case, assume towards a contradiction that

$$t_0 = \inf_{t>0}\{t \mid Q(t) < 0, S(t) < 0, \bar{S}(t) < 0, I(t) < 0 \text{ or } V(t) < 0\},$$

with $t_0 < \infty$.

Next, let $W = I + V$ and first assume that $\omega \geq \delta$. Then

$$W' = -\omega W + (\alpha - \delta + \omega) I.$$

If $f(t) = (\alpha - \delta + \omega) I$, then $f(t) \geq 0$ for $t \in [0, t_0]$. Second, assume that $\omega < \delta$. Then

$$W' = -\delta W + \alpha I + (\delta - \omega) V.$$

If $f(t) = \alpha I + (\delta - \omega) V$, then $f(t) \geq 0$ for $t \in [0, t_0]$. In general,

$$W' = -c_1 W + f(t), \tag{17}$$

for some $c_1 > 0 \in \mathbb{R}$ and with $f(t) \geq 0$ for $t \in [0, t_0]$. The solution of Equation (17) is

$$W(t) = W(0)\, \mathrm{e}^{-c_1 t} + \mathrm{e}^{-c_1 t} \int_0^t \mathrm{e}^{c_1 \xi} f(\xi)\, \mathrm{d}\xi.$$

If $W(0) = 0$, the system reduces to the model with no treatment. Otherwise, because $W(0) > 0$ and $f(t) \geq 0$, $W(t) > 0$ for $t \in [0, t_0]$. Since $W(t_0) > 0$, $N(t_0) > 0$. With $N(t_0) > 0$, we can now show that all compartments stay non-negative.

We begin with the age-structured PDE, Equation (14), and show that $\hat{S}(\tau, t) \geq 0$ for $t \in [0, t_0 + \eta)$, where $\eta = \min\{\epsilon, \tau\}$. For each $\zeta \in \mathbb{R}$, define

$$S_\zeta^*(T) = \hat{S}(\zeta + T, T).$$

We are going to find solutions along the characteristic lines, $x = \zeta + T$ with $t = T$. Then,

$$\frac{\mathrm{d}S_\zeta^*}{\mathrm{d}T} = \frac{\partial \hat{S}}{\partial x} + \frac{\partial \hat{S}}{\partial t}$$

and

$$(S_\zeta^*)' = -d_3 S_\zeta^* - \kappa \frac{V S_\zeta^*}{N}.$$

For each ζ, Equation (14) has now been converted into an ODE.

Since $t = T$,

$$S_\zeta^{*'}(t) = -d_3 S_\zeta^*(t) - \kappa \frac{V(t) S_\zeta^*(t)}{N(t)}.$$

Letting $g(t) = d_3 + \kappa V(t)/N(t)$, we obtain

$$S_\zeta^{*'}(t) = -g(t) S_\zeta^*(t). \tag{18}$$

Replacing Equation (14) with Equation (18), we have a system of ODE's along each characteristic line. From the form of the system of equations, and the non-negativity of the initial conditions assumption, $t_0 > 0$.

Since $N(t_0) > 0$, then the ODE system is well posed and a solution exists on an interval $(t_0 - \epsilon, t_0 + \epsilon)$. Moreover, by continuity, we may assume $N(t) > 0$ for $t \in (t_0 - \epsilon, t_0 + \epsilon)$.

Then solutions of Equation (18) along the characteristic lines $x = \zeta + t$ are

$$S_\zeta^*(t) = S_\zeta^*(0)\, \mathrm{e}^{-\int_0^t g(u)\,\mathrm{d}u}.$$

Each characteristic line in the $x - t$ plane intersects either the non-negative x-axis or the positive t-axis. If $\zeta \geq 0$, then the characteristic line intersects the non-negative x-axis and $S_\zeta^*(0) = \hat{S}(\zeta, 0)$, which is non-negative by assumption. Otherwise, $\zeta < 0$, the characteristic line intersects the positive t-axis at $-\zeta$, and $S_\zeta^*(0) = \hat{S}(0, -\zeta) = a_2 S(-\zeta)$. By the definition of t_0, we know that $S(-\zeta)$ is non-negative when $-\zeta \in [0, t_0]$. Thus, $S_\zeta^*(0) \geq 0$ for each characteristic line which intersects the positive t-axis at or below t_0, $(\zeta \geq -t_0)$.

Since $g(t)$ is bounded $(0 \leq g(t) \leq d_3 + \kappa)$ and $S_\zeta^*(0) \geq 0$ for $\zeta \geq -t_0$, on the corresponding characteristic lines $S_\zeta^*(t)$ will remain non-negative for as long as the solution exists. Therefore, $\hat{S}(\tau, t)$ will remain non-negative as well, for $t \in (t_0 - \eta, t_0 + \eta)$ where $\eta = \min\{\epsilon, \tau\}$. η is defined this way to ensure that solutions lie on the proper characteristic lines and that solutions exist.

Next, we evaluate Equations (12)–(16), excluding the PDE. Each of the four equations is of the form $B'(t) = A(t) - r(t)B(t)$, and $B = Q$, S, I, or V. Each equation has a solution of the form

$$B(t) = B(0)\, \mathrm{e}^{-\int_0^t r(s)\,\mathrm{d}s} + \int_0^t \mathrm{e}^{-\int_\xi^t r(s)\,\mathrm{d}s} A(\xi)\,\mathrm{d}\xi,$$

where B is either Q, S, I or V. For Equation (12), $A(t) = 2\hat{S}(\tau, t)$. We know $\hat{S}(\tau, t)$ is greater than or equal to zero for $t \in [0, t_0 + \eta)$, from the earlier characteristics argument. By assumption, $Q(0) \geq 0$ and we see that $Q(t) \geq 0$ for $t \in (t_0 - \eta, t_0 + \eta)$. For Equation (13), $A(t) = a_1 Q(t)$, so by similar reasoning, $S(t) \geq 0$ for $t \in (t_0 - \eta, t_0 + \eta)$. Since $S(t) \geq 0$ for $t \in (t_0 - \eta, t_0 + \eta)$, $S_\zeta^*(0) \geq 0$ for characteristic lines intersecting the t-axis up to $t_0 + \eta$. So, $\hat{S}(x, t) \geq 0$ for $t \in (t_0 - \eta, t_0 + \eta)$, and therefore so is $\bar{S}(t)$. Finally, since $Q, S, \hat{S} \geq 0$, using the same arguments that were used to explain non-negativity of solutions in Section 2.1.2, solutions cannot leave the positive quadrant of the I–V plane and I and V will remain non-negative for $t \in (t_0 - \eta, t_0 + \eta)$.

We have shown that all compartments remain non-negative for $t \in (t_0 - \eta, t_0 + \eta)$. This contradicts the definition of t_0. We conclude that solutions remain non-negative for all time. ■

3. Numerical results

3.1. *Parameter sensitivity analysis*

To study the effects of variations in parameters on model behaviour, we use the Latin hypercube sampling (LHS) [17]. Such a study is useful for statistically determining which parameters are

Table 1. Table of parameters varied in LHS simulations of the full model, given by Equations (12)–(16).

Parameter	Description	Range	Reference	SROC	p-value
a_1	Quiescent cell entrance into active phases (day^{-1})	$0.9 \pm 50\%$	[16]	-0.2262	5×10^{-13}
a_2	Active cell entrance into quiescence (day^{-1})	$0.6 \pm 50\%$	[16]	0.1125	0.0004
d_1	Quiescent cell death (day^{-1})	$1 \times 10^{-5} \pm 50\%$	[16]	0.0092	0.7724
d_2	Active cell death (day^{-1})	$0.15 \pm 50\%$	[16]	-0.0419	0.1852
α	Virion production (day^{-1})	$3 \pm 50\%$	Variable	-0.1391	1×10^{-5}
δ	Infected cell elimination (day^{-1})	$1.119 \pm 50\%$	[3]	0.0065	0.8379
ω	Free virion decay (day^{-1})	$0.3 \pm 50\%$	[3]	0.0267	0.3987
τ	Minimum duration of active phases (day)	[0, 3]	Variable	-0.0633	0.0455
κ	Kinetic coefficient (day^{-1})	[0, 5]	Variable	-0.3610	4×10^{-32}

Notes: Parameters are varied around their estimated values, which were obtained from the references cited in the fourth column. The third column reports SROCs between randomized parameter values and the resulting cancer concentration at time $t = 100$ days. For all simulations, it was assumed that $d_3 = d_2$.

most dynamically influential. LHS involves numerically solving the system of equations multiple times with randomly sampled parameter values. The samples are chosen such that each parameter is well distributed over its range of admissible values.

In this study, we conduct 1000 LHS simulations of the full model, given by Equations (12)–(16), and vary all model parameters according to a uniform distribution over the ranges shown in Table 1. For each simulation, we measure the tumour burden given by $Q + S + \bar{S} + I$ to determine whether or not virotherapy is able to control the growth of the tumour over this time frame. To assess the influence of each parameter, we calculate the Spearman rank-order correlation (SROC) of each parameter and the tumour burden at 100 days after the start of treatment.

From the results displayed in Table 1, we see that the tumour burden (measured at time $t = 100$ days) is most negatively correlated with the following parameters: a_1 – the rate at which quiescent cells enter the active phase, α – the rate at which virions are produced from the lysis of infected cells, and κ – the kinetic coefficient that governs the rate of interaction between virions and cells. The tumour burden is also significantly negatively correlated with τ – the minimum duration of the active phases of the cell cycle. These results imply that cells which spend more time in active phases of the cell cycle are more susceptible to the effects of virotherapy. In addition, viruses that produce more virions and infect cells at a faster rate tend to drive the cancer level lower.

On the other hand, the tumour burden is strongly positively correlated with a_2, the rate at which active cells enter quiescence. This result complements the strong negative correlation with a_1 because it implies that cells that are only active for a brief period of time before returning to quiescence render themselves less susceptible to virotherapy. The remaining parameters, d_1, d_2, δ, and ω, pertain to death and decay rates of cells and virions and have little correlation with the tumour burden.

These results imply that from a treatment perspective, it is strategic to combine a strong virus therapeutic with a drug that prolongs the progression of cancer cells through the active cell cycle. We direct the reader to the discussion section for commentary on synergy between cell cycle altering drugs and VSV, and how this interaction can be incorporated into our model.

3.2. *Therapy trajectories and dual parameter analysis*

3.2.1. *Non-delay case*

Figure 2 shows three plots: the plot on the left displays unabated tumour growth over time. The plot on the right exhibits the effect of VSV treatment on tumour growth over time. Essentially, the untreated tumour grows exponentially (Figure 2, left). However, after treatment with VSV,

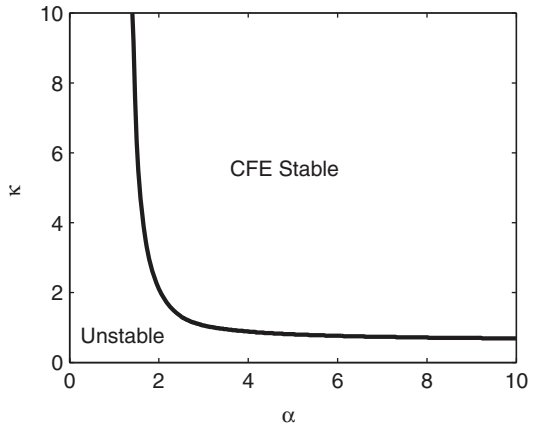

Figure 3. Stability map for parameters governing viral reproduction (α) and contact (κ). Other parameter values are the same as in Figure 2.

the tumour is eliminated over time, and the solution approaches the CFE (Figure 2, right). If transmission were modelled with mass action instead of ratio dependence, the solution would oscillate indefinitely (Figure 2, middle).

Two parameters that are strongly correlated with the effectiveness of VSV treatment are α and κ. As α increases, viral reproduction increases, and more virions are released by each cell that is infected and lysed. Increasing the amount of viral particles increases the likelihood of virus–cell contact, resulting in a more effective treatment. As κ increases, the likelihood that any susceptible cell will become infected increases, also resulting in more effective therapy. Figure 3 shows how the two parameters interact to either result in stability or instability of the CFE. Interestingly, as α decreases, the increase in the transmission rate needed to fully remove the tumour grows exponentially. As α decreases below 2, κ becomes prohibitively large, rendering the treatment ineffective, even if it were possible to affect the transmission rate. The same statement can be made for low values of κ. As the transmission rate becomes small, the viral reproduction rate needed to wipe out the tumour becomes unreasonably large. Therefore, VSV must reproduce at a sufficient rate *and* be reasonably transmissible for the treatment to remove the entire tumour population.

3.2.2. *Delay case*

Figure 4 illustrates how the delay value, or the minimum duration of the susceptible state, can increase the efficacy of the virus. In the left panel, the delay is considered without VSV treatment. Under these parameters, the tumour grows exponentially. In the middle panel, using the same parameters for tumour growth, the tumour is treated with VSV, but the delay is not taken into account. Again, the tumour grows exponentially. However, once the time delay is included, VSV successfully eliminates the tumour (right panel), demonstrating how the delay and the treatment interact, leading to successful eradication of the tumour.

Next, we study how three parameters determining the efficacy of VSV treatment, α, κ, and τ, interact (Figure 5). First, the stability of the CFE, while varying α and κ, with $\tau = 1$ day is considered (Figure 5, left). The rest of the parameter values are the same as those used in the study of the non-delay model. The parameters qualitatively interact in the same manner as in the non-delay model, but the curve is shifted downward and to the left, showing that, due to the delay, the treatment is effective for a wider range of both α and κ values. Next, α and τ are varied, while

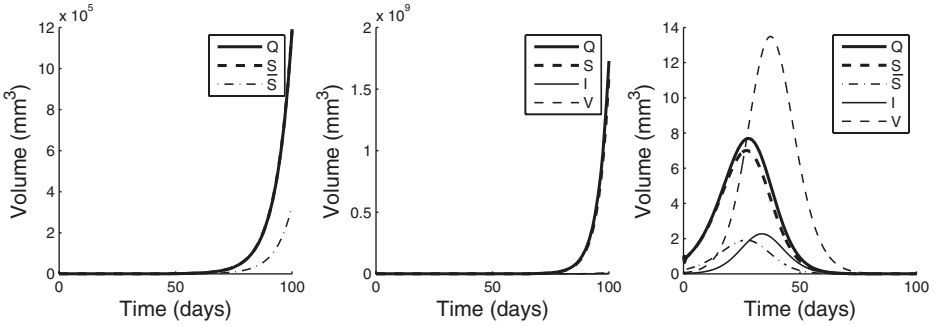

Figure 4. Left: uncontrolled tumour growth (in the absence of virotherapy) under prolonged cell cycle progression ($\tau = 0.5$). Middle: when $\kappa = 0.8$, virotherapy treatment fails; minimum cell cycle time course is not accounted for. Right: when $\kappa = 0.8$, virotherapy with a minimum cycling time ($\tau = 0.5$) results in a stable cancer-free state. All other parameter values are the same as in Figure 2.

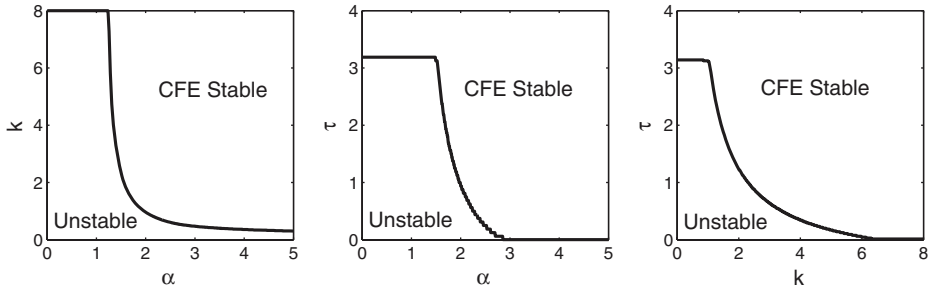

Figure 5. α, κ, and τ are varied, two at a time. For small α and κ, a delay value (τ) beyond a certain threshold will ensure stability of the origin. Parameter values if not varied: $a_1 = 0.9$, $a_2 = 0.6$, $d_1 = 0.00001$, $\delta = 1.119$, $\omega = 0.3$, $\alpha = 1.5$, $\kappa = 1$, and $\tau = 1$.

keeping $\kappa = 1$ (Figure 5, middle). The curve plateaus at the maximum value on the left. The minimum value of τ needed for stability is determined in Theorem 2.2, and is not dependent on α or κ. As α increases, the length of τ necessary to cause stability, decreases and approaches zero as we reach the value of α necessary to cause stability without the delay (shown in the corresponding picture for the non-delay model). Finally, κ and τ are varied, while keeping $\alpha = 1.5$ (Figure 5, right). The results are qualitatively similar to varying α and τ, except scaled.

4. Discussion

It was reported in 1904 that a patient's cancer was driven into remission due to a viral infection [12]. Over a century later, a complete understanding of the underlying dynamics of the viral treatment of tumours is still lacking, but some determinants of successful treatment have been uncovered. For example, the success of virotherapy is heavily dependent on the particular virus chosen to treat the tumour cells of interest. VSV has demonstrated anti-tumour efficacy in a large panel of human tumour cell lines. Although VSV treats many types of tumours, experimental observations in leukemic T-lymphocytes suggest that VSV does not kill non-proliferating tumour cells [19]. Seeking a better understanding of the dynamics of cell cycle-dependent oncolytic viruses, we have developed a custom-tailored mathematical model for treatment with the oncolytic VSV therapeutic, which captures its cell cycle-specific action. The model consists of a system of differential equations, which include a representation of the non-quiescent phases of the cell cycle as a process

with a minimum biological time course. We found that the parameters governing virotherapy treatment, as well as the delay, affect the global asymptotic behaviour of our model; biologically, initiation of therapy and cell cycle-specific effects both impact the long-term behaviour of the tumour.

We began with a framework for studying simple tumour growth with a seed model containing compartments for resting and proliferating cells. Linear systems analysis yielded the expected determinants of tumour growth and remission, which depend solely on cell transfer and death rates. When we extended the model to account for the minimum biological time course of the phases of the cell cycle leading to and including mitosis, we arrived at a three-dimensional system of DDEs. In the context of the cell cycle, the delay value, τ, is the minimum amount of time tumour cells must spend in the non-quiescent phases of the cell cycle. We found that for a given set of model parameters, there exists a minimum value of τ that will drive the system towards a globally stable cancer-free state. Furthermore, this threshold value can be calculated in terms of the growth and death rates of tumour populations.

From the original model of tumour growth without the delay, we introduced virotherapy treatment by including two additional compartments: infected cells and free virions. Virus-cell contact and virus production, occurring via the lytic cycle, were included in the model. These kinetics are modelled through the ratio-dependent contact between free virions and tumour cells. Some models of virotherapy have utilized mass action kinetics to model virus–cell contact [3,30]. While mass action permits exact linear systems analysis, it yields a model in which therapy does not impact the stability of the CFE. This result does not completely reveal the underlying strength of virotherapy that has been demonstrated in many experiments: viral injections can indeed yield tumour-free states. Our model complements these experimental results; the initiation of virotherapy treatment in our model can drive the system towards the CFE. In addition, through our five-dimensional age-structured model, we studied how the parameters that govern the lytic cycle operate together, leading to tumour elimination. As any such parameter becomes small, successful therapy becomes unattainable, as exponential growth in the other parameter is needed.

In our full model, we included a holding state for cells which enter the active stages of the cell cycle, as developed in our three-dimensional delayed model of tumour growth but this time using an age-structured PDE model. The holding state allows us to properly account for cell death and viral infection over the length of the delay, while also guaranteeing non-negativity of solutions. For parameters producing therapeutic failure (exponential tumour growth), a cancer-free state can be attained for combinations of treatment parameters and the delay value. Parameter sensitivity analysis illustrated that the rate of intracellular viral replication, α, the coefficient for virus–cell contact, κ, the rate of entry into the susceptible phase from quiescence, a_1, the rate of entry into quiescence from the susceptible phase, a_2, and the time delay, τ, substantially impact model behaviour. Sampling of two-dimensional parameter space demonstrated that the values of α, κ, and τ must be sufficiently large to ensure stability of the CFE. Therefore, the model demonstrates the importance of abundant virus–cell fusion, rapid replication, and prolonged cell cycle progression. Owing to the presence of a broadly neutralizing immune response after initial use of VSV, it is essential to optimize the aforementioned factors in order to maximize the impact of a single treatment [6].

The interaction between the virus therapeutic, cancerous cell populations, and their environment is complex. Our model simplifies many facets of this system, while retaining features which reveal dynamic behaviour. For example, we represent tumour and virion populations as functions of time. In reality, tumours are spatially complex entities with elaborate growth patterns and vasculature. Also, viral particle reproduction and flow within a tumour are not necessarily uniform. Although our model does not account for these multi-scale biological features, we find that it functions as a suitable framework for the holistic study of virus and cell population dynamics. It is also a sound baseline model, to which other important physical features may be added. For example, our model

can be modified to explore the effects of radiotherapy or chemotherapy coupled with virotherapy treatment. Of particular interest is the synergistic relationship between VSV and chemotherapy agents such as aphidicolin and paclitaxel [19]. These drugs arrest tumour cells during the active phases of the cell cycle, increasing the probability of successful VSV attack over the entire tumour population [19]. In the context of our model, this can be interpreted as an increased delay value, yielding less stringent constraints on other parameters of the model for the achievement of a cancer-free state. Overall, while we present a simplified representation of virotherapy within a human host, our model is robust and adaptable.

There is visible progress in the development and testing of oncolytic virus therapeutics. A large body of theoretical, experimental and clinical work has been initiated in the past several years. Notably, several ground-breaking Phase III trials have begun. Although therapeutic development strongly depends on animal models and tests on human subjects, mathematical modelling navigates ground that is experimentally inaccessible. Specifically, mathematical models such as ours can pinpoint the causes of therapeutic stagnation or failure. Such insights complement the efforts of physicians and experimental scientists in their development of novel cancer therapies.

Acknowledgement

We thank Gieri Simonett for his comments on the manuscript. J.F. was supported in part by an AMS-Simons Travel Grant.

References

[1] G.G. Au, A.M. Lindberg, R.D. Barry, and D.R. Shafren, *Oncolysis of vascular malignant human melanoma tumors by Coxsackievirus A21*, Int. J. Oncol. 26 (2005), pp. 1471–1476.
[2] Z. Bajzer, T. Carr, D. Dingli, and K. Josic, *Optimization of tumor virotherapy with recombinant measles virus*, in *Optimization in Medicine and Biology*, G.J. Lim and E.K. Lee, eds., Auerbach Publications, New York, 2008.
[3] Z. Bajzer, T. Carr, K. Josic, S.J. Russell, and D. Dingli, *Modeling of cancer virotherapy with recombinant measles viruses*, J. Theor. Biol. 252 (2008), pp. 109–122.
[4] S. Balachandran and G.N. Barber, *Vesicular stomatitis virus (VSV) therapy of tumors*, IUBMB Life 50 (2000), pp. 135–138.
[5] G.N. Barber, *VSV-tumor selective replication and protein translation*, Oncogene 24 (2005), pp. 7710–7719.
[6] J. Bell, K. Parato, and H. Atkins, *Vesicular stomatitis virus*, in *Viral Therapy of Cancer*, K.J. Harrington, R.G. Vile, and H.S. Pandha, eds., Wiley, Hoboken, NJ, 2008.
[7] F. Berezovsky, G. Karev, B. Song, and C. Castillo-Chavez, *A simple epidemic model with surprising dynamics*, Math. Biosci. Eng. 2 (2005), pp. 133–152.
[8] M. Biesecker, J.H. Kimn, H. Lu, D. Dingli, and Z. Bajzer, *Optimization of virotherapy for cancer*, Bull. Math. Biol. 72 (2010), pp. 469–489.
[9] C. Colijn and M.C. Mackey, *A mathematical model of hematopoiesis-I. Periodic chronic myelogenous leukemia*, J. Theor. Biol. 237 (2005), pp. 117–132.
[10] C. Comins, J. Spicer, A. Protheroe, V. Roulstone, K. Twigger, C.M. White, R. Vile, A. Melcher, M.C. Coffey, K.L. Mettinger, G. Nuovo, D.E. Cohn, M. Phelps, K.J. Harrington, and H.S. Pandha, *REO-10: A phase I study of intravenous reovirus and docetaxel in patients with advanced cancer*, Clin. Cancer Res. 16 (2010), pp. 5564–5572.
[11] D. Dingli, K.W. Peng, M.E. Harvey, P.R. Greipp, M.K. O'Connor, R. Cattaneo, J.C. Morris, and S.J. Russell, *Image-guided radiovirotherapy for multiple myeloma using a recombinant measles virus expressing the thyroidal sodium iodide symporter*, Blood 103 (2004), pp. 1641–1646.
[12] G. Dock, *The influence of complicating diseases upon leukaemia*, Amer. J. Med. Sci. 127 (1904), pp. 563–592.
[13] A. Friedman and Y. Tao, *Analysis of a model of a virus that replicates selectively in tumor cells*, J. Math. Biol. 47 (2003), pp. 391–423.
[14] C. Heise, A. Sampson-Johannes, A. Williams, F. McCormick, D.D. Von Hoff, and D.H. Kirn, *ONYX-015, an E1B gene-attenuated adenovirus, causes tumor-specific cytolysis and antitumoral efficacy that can be augmented by standard chemotherapeutic agents*, Nat. Med. 3 (1997), pp. 639–645.
[15] N.L. Komarova and D. Wodarz, *ODE models for oncolytic virus dynamics*, J. Theor. Biol. 263 (2010), pp. 530–543.
[16] W. Liu, T. Hillen, and H.I. Freedman, *A mathematical model for M-phase specific chemotherapy including the G0-phase and immunoresponse*, Math. Biosci. Eng. 4 (2007), pp. 239–259.
[17] M.D. McKay, W.J. Conover, and R.J. Beckman, *A comparison of three methods for selecting values of input variables in the analysis of output from a computer code*, Technometrics 21 (1979), pp. 239–245.

[18] A.S. Novozhilov, F.S. Berezovskaya, E.V. Koonin, and G.P. Karev, *Mathematical modeling of tumor therapy with oncolytic viruses: Regimes with complete tumor elimination within the framework of deterministic models*, Biol. Direct. 1 (2006). Available at http://www.biology-direct.com/content/1/1/6

[19] S. Oliere, M. Arguello, T. Mesplede, V. Tumilasci, P. Nakhaei, D. Stojdl, N. Sonenberg, J. Bell, and J. Hiscott, *Vesicular stomatitis virus oncolysis of T lymphocytes requires cell cycle entry and translation initiation*, J. Virol. 82 (2008), pp. 5735–5749.

[20] L.R. Paiva, C. Binny, S.C. Ferreira, and M.L. Martins, *A multiscale mathematical model for oncolytic virotherapy*, Cancer Res. 69 (2009), pp. 1205–1211.

[21] B.H. Park, T. Hwang, T.C. Liu, D.Y. Sze, J.S. Kim, H.C. Kwon, S.Y. Oh, S.Y. Han, J.H. Yoon, S.H. Hong, A. Moon, K. Speth, C. Park, Y.J. Ahn, M. Daneshmand, B.G. Rhee, H.M. Pinedo, J.C. Bell, and D.H. Kirn, *Use of a targeted oncolytic poxvirus, JX-594, in patients with refractory primary or metastatic liver cancer: A phase I trial*, Lancet Oncol. 9 (2008), pp. 533–542.

[22] A.L. Pecora, N. Rizvi, G.I. Cohen, N.J. Meropol, D. Sterman, J.L. Marshall, S. Goldberg, P. Gross, J.D. O'Neil, W.S. Groene, M.S. Roberts, H. Rabin, M.K. Bamat, and R.M. Lorence, *Phase I trial of intravenous administration of PV701, an oncolytic virus, in patients with advanced solid cancers*, J. Clin. Oncol. 20 (2002), pp. 2251–2266.

[23] L. Pujo-Menjouet and M.C. Mackey, *Contribution to the study of periodic chronic myelogenous leukemia*, CR Biol. 327 (2004), pp. 235–244.

[24] P.S. Reddy, K.D. Burroughs, L.M. Hales, S. Ganesh, B.H. Jones, N. Idamakanti, C. Hay, S.S. Li, K.L. Skele, A.J. Vasko, J. Yang, D.N. Watkins, C.M. Rudin, and P.L. Hallenbeck, *Seneca Valley virus, a systemically deliverable oncolytic picornavirus, and the treatment of neuroendocrine cancers*, J. Natl. Cancer Inst. 99 (2007), pp. 1623–1633.

[25] C.L. Reis, J.M. Pacheco, M.K. Ennis, and D. Dingli, *In silico evolutionary dynamics of tumour virotherapy*, Integr. Biol. (Camb) 2 (2010), pp. 41–45.

[26] T. Todo, R.L. Martuza, S.D. Rabkin, and P.A. Johnson, *Oncolytic herpes simplex virus vector with enhanced MHC class I presentation and tumor cell killing*, Proc. Natl. Acad Sci. USA 98 (2001), pp. 6396–6401.

[27] M. Tubiana and E. Malaise, *Comparison of cell proliferation kinetics in human and experimental tumors: Response to irradiation*, Cancer Treat. Rep. 60 (1976), pp. 1887–1895.

[28] M. Villasana and A. Radunskaya, *A delay differential equation model for tumor growth*, J. Math. Biol. 47 (2003), pp. 270–294.

[29] L.M. Wein, J.T. Wu, and D.H. Kirn, *Validation and analysis of a mathematical model of a replication-competent oncolytic virus for cancer treatment: Implications for virus design and delivery*, Cancer Res. 63 (2003), pp. 1317–1324.

[30] D. Wodarz, *Gene therapy for killing p53-negative cancer cells: Use of replicating versus nonreplicating agents*, Hum. Gene Ther. 14 (2003), pp. 153–159.

[31] J.T. Wu, H.M. Byrne, D.H. Kirn, and L.M. Wein, *Modeling and analysis of a virus that replicates selectively in tumor cells*, Bull. Math. Biol. 63 (2001), pp. 731–768.

[32] D. Xiao and S. Ruan, *Global dynamics of a ratio-dependent predator-prey system*, J. Math. Biol. 43 (2001), pp. 268–290.